

Identification and Active Disturbance Rejection for the JPL Phase B Test Bed *

D.B. Eldred
Jet Propulsion Laboratory
4800 Oak Grove Drive, MS 198-326
Pasadena, CA 91109

J.S. Gibson and Wu-Jeng Li
Mechanical, Aerospace, and Nuclear Engineering
University of California, Los Angeles 90024-1597

Abstract

Active disturbance rejection to minimize optical path length error is illustrated by experimental results from the JPL Phase B Test Bed, which incorporates an interferometric sensor and a controllable trolley mounted on a flexible truss structure. The controller actively isolates the optical instruments from structural vibrations induced by external disturbances consisting of linear combinations of sinusoidal signals.

1 Introduction

This paper describes the results of experimental implementation of a new disturbance-rejecting controller. The controller is based on a discrete time input-output model which is estimated from experimental data using an adaptive order lattice filter. Though implemented off-line in the experiment reported in this paper, the lattice filter is designed for real-time implementation in adaptive identification and control. The experimental results demonstrate that the disturbance-rejecting controller can reduce optical path length response by an order of magnitude, as compared to the response produced by the nominal stabilizing controller alone.

The controlled output in the experiment is the laser path length through an optical train on the JPL Phase B Testbed (Figure 1.1). The Testbed, developed to demonstrate sub-micron control technologies for future space missions, consists of a 2.5 m high truss structure constructed from aluminum tubing rigidly bolted to aluminum nodes. An optical compensation system is used to provide precise, high bandwidth control to the optical light path length, which is measured using a laser interferometer. It employs a primary and a secondary mirror configured as a retroreflector, and is isolated as a unit from the underlying truss structure by flexure pivots. Path length control for this experiment is achieved with both a voice-coil actuator which reacts between the truss structure and the optical compensation system, and a piezoelectric element which moves the secondary mirror with high bandwidth. A 68030-based real-time computer provides the computation required for the control laws. While the Phase B Testbed has provisions for using a variety of sensors and actuators including active struts and passive dampers, only the voice coil actuator is used for this experiment. Disturbance inputs are provided by a modal shaker attached to the truss structure along the vertical tower. Additional details can be found in [1, 2].

*This research was carried out by the Jet Propulsion Laboratory, California Institute of Technology, under a contract with the National Aeronautics and Space Administration.

2 Modeling and Identification

2.1 Models of Plant and Disturbance

Identification is based on the following SISO discrete-time input/output model of the structure:

$$a_p(q^{-1})y(t) = b_p(q^{-1})u(t) + d(t), \quad (2.1)$$

where $u(t)$, $y(t)$, and $d(t)$ are the control, output, and disturbance sequences, respectively, and

$$\begin{aligned} a_p(q^{-1}) &= 1 + a_1 q^{-1} + a_2 q^{-2} + \dots + a_{n_p} q^{-n_p}, \\ b_p(q^{-1}) &= b_1 q^{-1} + b_2 q^{-2} + \dots + \text{fir}_{n_b} q^{-n_b}. \end{aligned} \quad (2.2)$$

We assume that the disturbance satisfies

$$a_d(q^{-1})d(t) = \epsilon(t) \quad (2.3)$$

for some monic polynomial $a_d(q^{-1})$ of order n_d and some random noise sequence $\epsilon(t)$.

2.2 Identification

The identification experiment reported here consisted of forcing the plant with a known random control sequence $u(t)$ and recording input/output data at 100Hz. The control $u(t)$ was a zero order hold. In this experiment, the disturbance $d(t)$ was zero. A 111 unwindowed adaptive lattice filter developed in [3] was used to identify the plant polynomials $a_p(q^{-1})$ and $b_p(q^{-1})$, for a series of orders n , from the experimental input/output data.

The lattice filter used here has been used previously to identify a large flexible truss, as reported in [3, 4]. Like most lattice filters, the lattice in [3] generates recursive least-squares estimates of models of all orders up to some maximum order. A least-squares lattice filter is a fast, numerically robust algorithm for performing a Gram-Schmidt orthogonalization of the regression vectors in a linear autoregressive model. Lattice filters are numerically stable, efficient, and order-recursive. While classical least-squares algorithms require $O(n^2)$ operations at each time step, where n is the order of the model being identified, a lattice filter requires $O(n)$ operations at each time step. Also, a lattice filter generates least-squares estimates of models of all orders up to a maximum order N , thereby facilitating order-determination. Most lattice filters in the literature are prewindowed, which means that they assume that all initial data is zero. An unwindowed, or covariance lattice filter, provides the exact initialization for nonzero data. As illustrated in [5], a prewindowed lattice often takes much longer than an unwindowed lattice to converge to accurate parameter estimates when the initial data is not zero, as in the impulse response of a flexible structure. The multichannel unwindowed lattice filter developed in [3] eliminates numerical instabilities that can arise in standard lattices and in the lattice in [5] for large numbers of data channels.

For the experiment, models of orders between $n_p = 2$ and $n_p = 25$ were identified and compared. The frequency responses of all identified models for $20 \leq n_p \leq 25$ were indistinguishable. Figure 2.1 shows the bode amplitude plots for the models of orders 25, 7 (dash-dot curve), 2 (dashed curve). The models of orders 2 and 7 both capture the first mode of the plant (i.e., the trolley mode) very well. The model of order 7 also contains approximations to the second and third modes.

The JPL Phase B Testbed Structure

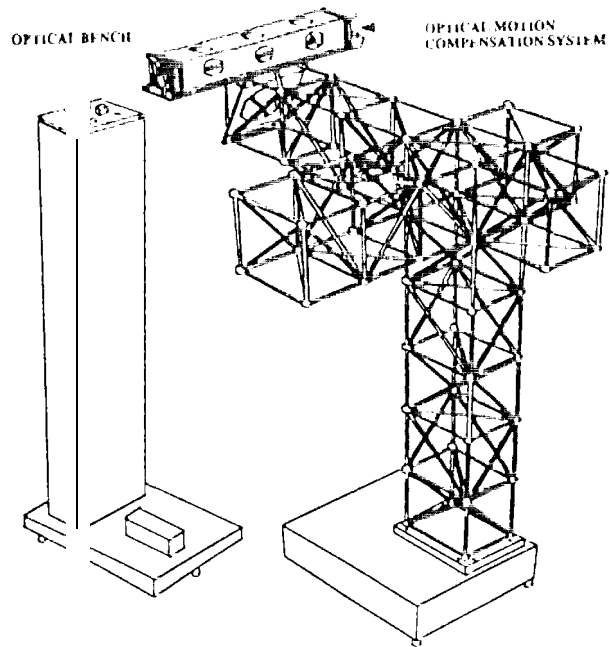


Figure 1.1

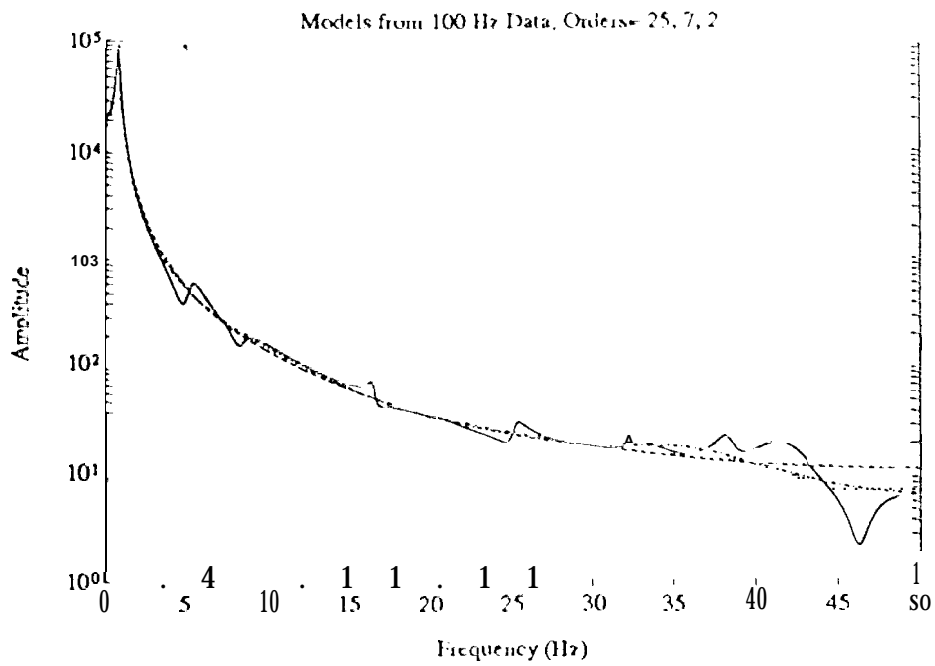


Figure 2.1

3 Controller Design

3.1 State-space Model of Plant and Disturbance

The controller design described here is from [6]. We let the variable t take integer values, and, for any function $x(t)$, we use standard notation for the forward shift operator: $(qx)(t) = x(t+1)$. We consider a linear system of the form

$$q \begin{pmatrix} x_p \\ x_d \end{pmatrix} = A \begin{pmatrix} x_p \\ x_d \end{pmatrix} + Bu, \quad (3.1)$$

$$y_1 = C_1 \begin{pmatrix} x_p \\ x_d \end{pmatrix} = [C_{11} \ C_{12}] \begin{pmatrix} x_p \\ x_d \end{pmatrix}, \quad (3.2)$$

$$y_2 = C_2 \begin{pmatrix} x_p \\ x_d \end{pmatrix} = [C_{21} \ C_{22}] \begin{pmatrix} x_p \\ x_d \end{pmatrix}, \quad (3.3)$$

with

$$A = \begin{bmatrix} A_p & A_{pd} \\ 0 & A_d \end{bmatrix}, \quad B = \begin{bmatrix} B_p \\ 0 \end{bmatrix}, \quad (3.4)$$

$$x_p(t) \in C^{n_p}, \quad x_d(t) \in C^{n_d}, \quad u(t) \in C^m, \quad y_1 \in C^r, \quad y_2 \in C^m. \quad (3.5)$$

The matrices A_p , B_p , A_d , C_i , and C_{ij} have the appropriate dimensions. We denote by X_p^1 the space of all complex $(n_p + n_d)$ -vectors x such the first n_p components of x are zero.

The controller designed in this section feeds back y_1 , the measured output, to make y_2 , the controlled output, zero. In applications like that in the following section, these two outputs will be the same.

Hypothesis 3.1

- i) (C_1, A) is detectable;
- ii) there exist matrices F_p and K_p such that

$$\hat{A}_p = A_p - F_p C_{11} \quad \text{and} \quad \tilde{A}_p = A_p - B_p K_p$$

are asymptotically stable and

$$\sigma(A_d) \cap (\sigma(\hat{A}_p) \cup \sigma(\tilde{A}_p)) = \emptyset;$$

- iii) $\det C_{21}(z - A_p)^{-1} B_p \neq 0 \quad \forall z \in \sigma(A_d)$.

For Conditions i) and ii), it is sufficient that (C_1, A) be observable, that (A_p, B_p) be controllable. Condition iii) says that no disturbance poles are transmission zeros of the plant.

3.2 Disturbance-rejecting Control Gain

Theorem 3.2 Under the hypotheses stated, there exists a unique pair of matrices $K_d(m \times n_d)$ and $\tilde{L}(n_p \times n_d)$ that satisfy the two matrix equations

$$\tilde{A}_p \tilde{L} - \tilde{L} A_d = B_p K_d - A_{pd} \quad (3.6)$$

and

$$C_{21} \tilde{L} + C_{22} = 0. \quad (3.7)$$

This matrix K_d is the unique $m \times n_d$ matrix K_d such that X_p^\perp is an unobservable subspace of $(C_2, A - BK)$ where

$$K = \begin{bmatrix} K_p & K_d \end{bmatrix}. \quad (3.8)$$

If

$$\hat{J} = \begin{bmatrix} I & \hat{L} \\ 0 & I \end{bmatrix}, \quad (3.9)$$

then

$$\hat{J}^{-1}(A - BK)\hat{J} = \begin{bmatrix} \hat{A}_p & 0 \\ 0 & A_d \end{bmatrix} \quad (3.10)$$

Proof That there is at most one K_d such that X_p^\perp is an unobservable subspace of $(C_2, A - BK)$ follows from the fact that no eigenvalues of A_d are transmission zeros of $C_{21} (2 - \hat{A}_p)^{-1} B_p$. The uniqueness of the solution pair K_d and \hat{L} for (3.6) and (3.7) then follows from the fact that (3.6) has a unique solution \hat{L} for each K_d , since \hat{A}_p and A_d have no common eigenvalues.

We adopt the following notation for a matrix M : $M_{i,j}$ denotes the i, j element of M , and $M_{:,j}$ denotes the j th column of M .

To prove existence of K_d and \hat{L} , we assume without loss of generality that A_d is in Schur form and that the eigenvalues of A_d are $\mu_j (j=1, \dots, n_d)$. In this case, the columns of K_d and \hat{L} are given recursively by

$$K_{d,j} = [C_{21}(\mu_j - \hat{A}_p)^{-1} B_p]^{-1} (C_{21}((\mu_j - \hat{A}_p)^{-1} (A_{pd,j} - \sum_{i=1}^{j-1} A_{d,ij} \hat{L}_{:,i}) - C_{22,j})), \quad (3.11)$$

$$\hat{L}_{:,j} = (\mu_j - \hat{A}_p)^{-1} (B_p K_{d,j} - A_{pd,j} + \sum_{i=1}^{j-1} A_{d,ij} \hat{L}_{:,i}), \quad (3.12)$$

with $A_{d,i0} = 0$ and $\hat{L}_{:,0} = 0$. \square

3.3 Estimator for State and Disturbance

We let \hat{L} be the unique $(n_p \times n_d)$ matrix that satisfies

$$\hat{A}_p \hat{L} - \hat{L} A_d = F_p C_{12} - A_{pd}, \quad (3.13)$$

and we define

$$\hat{J} = \begin{bmatrix} I & \hat{L} \\ 0 & I \end{bmatrix}. \quad (3.14)$$

Then

$$\hat{J}^{-1}(A - \begin{bmatrix} F_p \\ 0 \end{bmatrix} C_1)\hat{J} = \begin{bmatrix} \hat{A}_p & 0 \\ 0 & A_d \end{bmatrix}. \quad (3.15)$$

Since (C, A) is detectable, $(C_1 \hat{J}, \hat{J}^{-1}[A - \begin{bmatrix} F_p \\ 0 \end{bmatrix} C_1] \hat{J})$ and $(C_{11} \hat{L} + C_{12}, A_d)$ are detectable. Hence there exists an $n_d \times r$ matrix F_d such that

$$\hat{A}_d = A_d - F_d (C_{11} \hat{L} + C_{12}) \quad (3.16)$$

is asymptotically stable.

Next, we define

$$F = \begin{bmatrix} [F_p + \hat{L} F_d] \\ F_d \end{bmatrix} = \begin{bmatrix} F_p \\ 0 \end{bmatrix} + \hat{J} \begin{bmatrix} 0 \\ F_d \end{bmatrix}. \quad (3.17)$$

Then

$$\hat{J}^{-1}(A - FC_1)\hat{J} = \begin{bmatrix} \hat{A}_p & 0 \\ I - F_d C_{11} & \hat{A}_d \end{bmatrix}, \quad (3.18)$$

so that

$$q \begin{pmatrix} \hat{x}_p \\ \hat{x}_d \end{pmatrix} = (A - FC_1) \begin{pmatrix} \hat{x}_p \\ \hat{x}_d \end{pmatrix} + Bu + Fy_1 \quad (3.19)$$

is an asymptotically convergent observer for $\begin{pmatrix} x_p \\ x_d \end{pmatrix}$.

3.4 Controller and Closed-loop System

We define the controller for the system (3.1)-(3.3) by

$$u = -K \begin{pmatrix} \hat{x}_p \\ \hat{x}_d \end{pmatrix}, \quad (3.20)$$

$$q \begin{pmatrix} \hat{x}_p \\ \hat{x}_d \end{pmatrix} = A_{ctr}^{(pd)} \begin{pmatrix} \hat{x}_p \\ \hat{x}_d \end{pmatrix} + Fy_1, \quad (3.21)$$

$$A_{ctr}^{(pd)} = A - FC_1 - BK. \quad (3.22)$$

We will denote this controller by $(A', A_{ctr}^{(pd)}, F)$.

To illuminate the structure of this controller and the closed-loop system that it produces, we define the additional controller state matrix

$$A_{ctr}^{(p)} = A_p - B_p K_p - F_p C_{11} \quad (3.23)$$

and the closed-loop matrices

$$A^{(pd;pd)} = \begin{bmatrix} A & -BK \\ FC_1 & A_{ctr}^{(pd)} \end{bmatrix}, \quad (3.24)$$

$$A^{(p;pd)} = \begin{bmatrix} A_p & -B_p K \\ F_p C_{11} & A_{ctr}^{(pd)} \end{bmatrix}, \quad (3.25)$$

$$A^{(p;p)} = \begin{bmatrix} A_p & -B_p K_p \\ F_p C_{11} & A_{ctr}^{(p)} \end{bmatrix} \quad (3.26)$$

We refer to the controller $(K_p, A_{ctr}^{(p)}, F_p)$ as the basic stabilizing controller for the plant, and we have the common result

$$\sigma(A^{(p;p)}) = \sigma(\hat{A}_p) \cup \sigma(\hat{A}_p). \quad (3.27)$$

We refer to the closed-loop system that contains all of the states x_p , x_d , \hat{x}_p , and \hat{x}_d as the complete closed-loop system. The system matrix for the complete closed-loop system is $A^{(pd;pd)}$. The system matrix for the closed-loop system that contains the states x_p , \hat{x}_p , and \hat{x}_d is $A^{(p;pd)}$.

Next we define

$$J^{(p;p)} = \begin{bmatrix} I(n_p \times n_p) & 0 \\ I & I(n_p \times n_p) \end{bmatrix}, \quad J^{(p;pd)} = \begin{bmatrix} J^{(p;p)} & 0 \\ 0 & I(n_d \times n_d) \end{bmatrix} \quad (3.28)$$

$$J^{(pd;pd)} = \begin{bmatrix} I(n \times n) & 0 \\ I & I(n \times n) \end{bmatrix}, \quad (3.29)$$

where $n = n_p + n_d$. We have then

$$A^{(p;pd)} J^{(p;pd)}, \quad J^{(p;pd)} \begin{bmatrix} \hat{A}_p & -B_p K \\ 0 & (A - FC_1) \end{bmatrix}, \quad (3.30)$$

$$A^{(pd;pd)} J^{(pd;pd)} = J^{(pd;pd)} \begin{bmatrix} (A - BK) & -BK \\ 0 & (A - FC_1) \end{bmatrix} \quad (3.31)$$

It follows from (3.10), (3.18), (3.31), and (3.30) that

$$\sigma(A^{(p;pd)}) = \sigma(\hat{A}_p) \cup \sigma(\hat{A}_p) \cup \sigma(\hat{A}_d), \quad (3.32)$$

$$\sigma(A^{(pd;pd)}) = \sigma(A^{(p;pd)}) \cup \sigma(A_d). \quad (3.33)$$

It follows from Theorem 3.2 and (3.31) that, for all initial conditions, the $2(n_p + n_d)$ -dimensional state vector of the complete closed-loop system converges exponentially to the unobservable subspace of $([C_2 \ 0 \ 0], A^{(pd;pd)})$. For all states in this subspace, $\hat{x}_p = x_p$, $\hat{x}_d = x_d$, and $y_2 = 0$.

An illuminating equivalent realization of the controller in (3.20) (3.22) is

$$(K\hat{J}, \hat{J}^{-1}A_{ctr}^{(pd)}\hat{J}, \hat{J}^{-1}F) = \left(\begin{bmatrix} K_p & (K_p\hat{L} + K_d) \\ I - F_d C_{11} & \hat{A}_d \end{bmatrix}, \begin{bmatrix} A_{ctr}^{(p)} - B_p(K_p\hat{L} + K_d) \\ \hat{A}_d \end{bmatrix}, \begin{bmatrix} F_p \\ F_d \end{bmatrix} \right). \quad (3.34)$$

In this form, the controller that stabilizes the plant and rejects the disturbance consists of the basic stabilizing controller for the plant, coupled with the state estimator for the disturbance and a disturbance-rejecting control law.

If the measured output and controlled output are the same, then $C_1 = C_2$ and

$$\hat{J}^{-1}A_{ctr}^{(pd)}\hat{J} = \begin{bmatrix} [A_{ctr}^{(p)} + (\hat{L} - \hat{L})F_d C_{11} & 0 \\ -F_d C_{11} & \hat{A}_d \end{bmatrix}. \quad (3.35)$$

In this case then, the eigenvalues of A_d are eigenvalues of the controller, and for single-input and single-output, the eigenvalues of A_d are zeros of the closed-loop system consisting of the plant and the controller.

3.5 Numerical Design of the Controller

Here we discuss the computations required to construct the controller that stabilizes the plant and rejects the disturbance. We assume that the matrices in (3.1)–(3.4) are given. The following algorithm yields the controller in (3.8), (3.17), and (3.22). Whether this realization or some other (e.g., that in (3.34)) is used, the matrices that must be computed are F_p , K_p , \hat{L} , K_d , \hat{L} , and F_d .

Algorithm 3.3 (Controller Design)

- i) Determine matrices F_p and K_p such that Condition ii) of Hypothesis 9.1 holds.
- ii) Solve (9.6) and (9.7) for the matrices K_d and \hat{L} (by, for example, the recursive algorithm in (9.11) and (9.12)).
- iii) Solve (9.19) for the matrix L , and determine a matrix F_d such that the matrix A_d given by (3.16) is asymptotically stable.
- iv) For-in the matrices K , F , and $A_{ctr}^{(pd)}$ in (3.8), (3.17), and (3.22).

In this algorithm, Step i) is to design the basic stabilizing controller for the plant. This can be any stabilizing controller that includes an unbiased estimator for the plant state vector x_p . The design of the basic stabilizing controller for the plant is independent of the disturbance model, except that

the closed-loop poles produced by the basic controller should not be near any possible disturbance eigenvalues. This is not restrictive in applications where the disturbance is a linear combination of perhaps lightly damped sine waves.

Many classes of controllers can be used for the basic stabilizing controller for the plant, including LQG and LTR. For the experiment described in the next section, we use a combination of LQG design and pole placement to determine the control and estimator gains K_p and F_p . We note that H_∞ controllers do not fit directly into the design developed here for a disturbance-rejecting controller because they involve a biased estimator. The controller design in this paper can be extended to allow the basic stabilizing controller for the plant to be an H_∞ controller by using an unbiased auxiliary state estimator along with the H_∞ controller.

Steps ii)–iv) of Algorithm 3.3 construct the disturbance-rejecting part of the controller. It appears that one of the most, if not the most, efficient approach to solving (3.6) and (3.7) is to use the recursion in (3.11) and (3.12), especially with A_p as well as A_d in Schur (or quasi-Schur) form.

One of the most important features of the controller design here is that, once the basic stabilizing controller for the plant is determined, only Steps ii)–iv) of Algorithm 3.3 need be repeated if the disturbance changes. The resulting computational efficiency is especially important in adaptive disturbance rejection. Also, it follows from (3.32) that an erroneous disturbance model, as long as it has on eigenvalues in common with the basic closed-loop matrix $A^{(p;p)}$, will not cause the closed-loop system to be unstable.

3.6 State-space Model for the Experiment

In the experiment, we have $y_1 = y_2$ and $C_1 = C_2$; i.e., the measured output and controlled output are the same. For the matrices A_p, B_p , and C_{11} , we use the observer form corresponding to $a_p(q^{-1})$ and $b_p(q^{-1})$:

$$A_p = \begin{bmatrix} -a_1 & \mathbf{1} & \mathbf{0} & \dots & \mathbf{0} \\ -a_2 & 0 & 1 & \ddots & 0 \\ \vdots & \vdots & \vdots & \ddots & \vdots \\ -a_{n_p} & 0 & \dots & 0 & 1 \\ -a_{n_p} & 0 & \dots & 0 & 0 \end{bmatrix}, \quad B_p = \begin{bmatrix} b_1 \\ b_2 \\ \vdots \\ b_{n_p} \end{bmatrix}, \quad (3.36)$$

$$C_{11} = [1 \ 0 \ 0 \ \dots]$$

The $n_d \times n_d$ matrix A_d is constructed in the form

$$A_d = \begin{bmatrix} \Lambda_1 & 0 & \dots \\ 0 & \Lambda_2 & \ddots \\ \vdots & \vdots & \ddots \end{bmatrix}, \quad (3.37)$$

where each Λ_i is a real 2×2 matrix with eigenvalues equal to a complex-conjugate pair of disturbance poles (i.e., roots to $\mu^{n_d} a_d(\mu^{-1}) = 0$). Also,

$$A_{pd}(n_p \times n_d) = \begin{bmatrix} 1 \\ 0 \\ 0 \\ \vdots \end{bmatrix} [1 \ 0 \ 1 \ 0 \ \dots] = \begin{bmatrix} 1 & 0 & 1 & 0 & \dots \\ 0 & 0 & 0 & 0 & \dots \\ 0 & 0 & 0 & 0 & \dots \\ \vdots & \vdots & \vdots & \vdots & \vdots \end{bmatrix}. \quad (3.38)$$

4 control Results

The following table lists controllers used in the experiment. In each cam, the nominal controller is the controller that stabilizes the plant. The second-order and seventh-order nominal controllers were based, respectively, on the second-order and seventh-order models for which the frequency responses are plotted in Figure 2.2. The order of each disturbance-rejecting controller is the order of the nominal controller plus two orders for each disturbance frequency rejected.

Table 4.1: Controllers

Control Rate	Type of Controller	Order of Controller	Order of Nominal Controller	Frequencies Rejected
100 Hz	Stabilizing	2	2	"
100 Hz	DR	6	2	5 Hz & 10 Hz
100 Hz	Stabilizing	7	7	"
100 Hz	DR	11	7	5 Hz & 10 Hz
50 Hz	DR	6	2	5 Hz & 10 Hz
-50 Hz	DR	11	7	5 Hz & 10 Hz

DR: Disturbance-rejecting Controller

Figures 4.1- 4.8 compare time response of the laser path-length error produced by disturbance-rejecting controllers to either open-loop response or closed-loop response produced by controllers that only stabilize the plant. In these experiments, the disturbance consisted of various combinations of 5 Hz and 10 Hz sine waves, as noted in the figures.

In most cams, the disturbance-rejecting controllers based on the seventh-order model (i.e., the controllers of order 11) perform only marginally better than those based on the second-order model. As the figures indicate, the 100 Hz disturbance-rejecting controllers achieve an order-of-magnitude improvement in closed-loop response over open-loop and the stabilizing controllers only. However, the disturbance-rejecting controller does not eliminate the path-length error entirely, as the theory predicts. Figures 4.9-4.11 show typical powerspectral densities of the closed-loop responses. The dashed vertical lines lie at 5 Hz and 10 Hz. These figures show that the disturbance-rejecting controller does zero the output at the frequencies that the controller was designed to reject, but there exists residual closed-loop response at frequencies not present in the disturbance or the open-loop response.

There appear to be two possible explanations of the residual closed-loop response, both involving the discontinuous control command (i.e., the zero-order hold). One possibility is that the high-frequency content of the control excites lightly damped high frequency modes in the structure and the frequencies at which the power spectrum appears to be nonzero are aliases of the excited higher frequencies. The other possible source of the residual response is the discontinuous control command causes the voice-coil actuator to behave nonlinearly. Perhaps, further experiments should be conducted to determine the source of the residual response; however, whatever the explanation, the solution appears to be a smoother control sequence, produced either by a faster control rate or a low-pass filter on the control sequence. The amplitude of the residual response with the 100 Hz control rate is about one third of that with the 50 Hz control rate, and the 50 Hz controllers produce similar improvements over 25 Hz controllers. When the control rate increases from 50 Hz to 100 Hz, and similar improvement resulted when control rate increased from 25 Hz to 50 Hz. Thus, smoother control commands reduce the residual response.

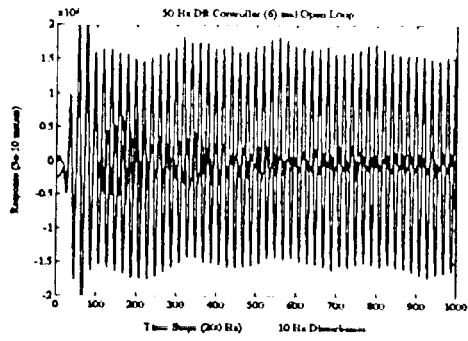


Figure 4.7

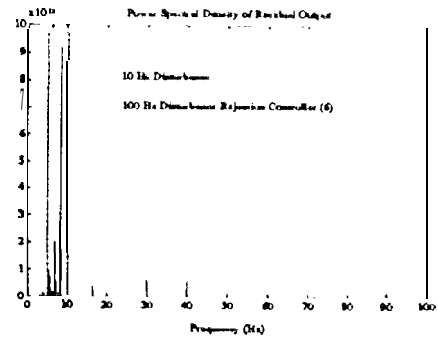


Figure 4.10

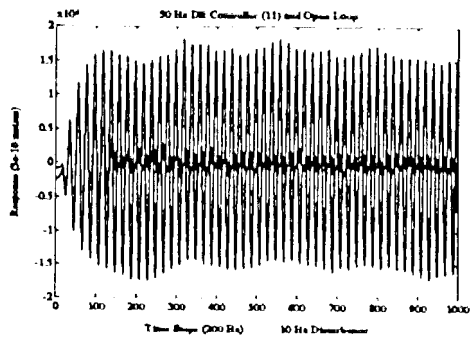


Figure 4.8

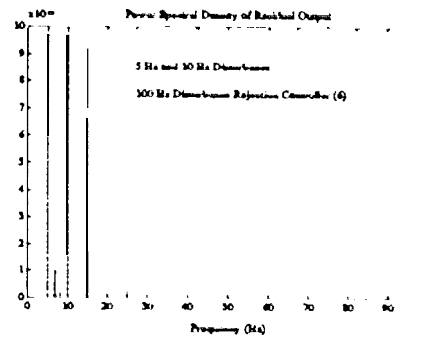


Figure 4.11

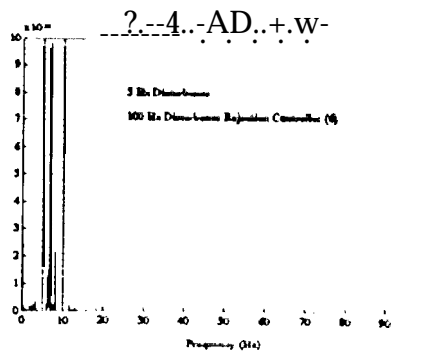


Figure 4.9

5 conclusions

The experimental results reported in this paper illustrate the ability of the disturbance-rejecting controller to suppress the effect of harmonic disturbances on a measured output. The experimental results suggest that faster sample-and-hold rates than those used for this paper will yield even better performance, approaching the theoretical performance where controlled output is zero. Indeed, the power spectra shown here for the 100 Hz controller show that the frequency content of the controlled output is very near zero at the frequencies that the controller is designed to reject.

To make the disturbance-rejecting controller adapt on-line to varying disturbances and/or plant dynamics, both the lattice filter and the control design must be run in real time on a laboratory computer, as simulated in [6]. The control design proposed in [6] and used for this paper can be used for efficient redesign of the disturbance-rejecting part of the controller when the disturbance changes.

References

- [1] M. O'Neal, D. Eldred, D. Liu, , and D. Redding, "Experimental verification of nanometer level optical pathlength control on a flexible structure," *Proceedings of the 4th NASA/DoD Controls/Structures Interaction Technology Conference*, November 1990.
- [2] D. Eldred and M. O'Neal, "The jpl phase b testbed facility," *Proceedings of the ADPA/AIAA/ASME/SPIE Active Materials and Adaptive Structures Conference*, November 1991.
- [3] S.-B. Jiang, *Unwindowed Multichannel Lattice Filters and Applications in Adaptive Identification and Control*. PhD thesis, University of California, Los Angeles, 1992.
- [4] S.-B. Jiang, J.S. Gibson, and J.J. Hollkamp, "Identification of a flexible structures by a new multichannel lattice filter," in *American Control Conference*, (Chicago), pp. 1681-1685, IEEE, June 1992.
- [5] S.-W. Chen and J.S. Gibson, "A new unwindowed lattice filter for RLS estimation," *IEEE Transactions on Signal Processing*, vol. 40, pp. 2158-2165, September 1992.
- [6] W.-J. Li and J.S. Gibson, "Adaptive identification and disturbance rejection for flexible structures," *submitted, 1992*.